ANTICANCER RESEARCH *40*: 653-664 (2020)
doi:10.21873/anticanres.13995

PGC-1α Regulates Cell Proliferation and Invasion *via* AKT/GSK-3β/β-catenin Pathway in Human Colorectal Cancer SW620 and SW480 Cells

SEONG-HOON YUN and JOO-IN PARK

Department of Biochemistry, Dong-A University College of Medicine, Busan, Republic of Korea

Abstract. *Background/Aim: Peroxisome proliferator-activated receptor γ coactivator 1α (PGC-1α) is a master regulator of mitochondrial biogenesis and metabolism. We investigated the effect of PGC-1α knockdown in the human colorectal cancer cell line SW620, which highly expresses PGC-1α. Materials and Methods: We established the PGC-1α shRNA-silenced SW620 stable cell line (PGC-1α shRNA-SW620 cells) and examined cell proliferation by cell counts and carboxyfluorescein succinimidyl ester (CFSE) staining, migration by wound-healing and transwell migration assay, and invasion by transwell assays. Results: PGC-1α knockdown inhibited cell proliferation, migration, and invasion in SW620 cells. Western blot analysis showed that p-AKT, p-GSK-3β, β-catenin, N-cadherin and vimentin expression were all reduced, but E-cadherin had increased expression in PGC-1α shRNA-SW620 cells. We also examined cell proliferation, migration, invasion and the expression of p-AKT, p-GSK-3β, β-catenin, N-cadherin, vimentin, and E-cadherin in PGC-1α overexpressing SW480 cells (a low PGC-1α expressing line). We observed a complete reversal of the results seen in the knockdown. Conclusion: PGC-1α might regulate cell proliferation and invasion via AKT/GSK-3β/β-catenin pathway in SW620 and SW480 cells.*

Colorectal cancer (CRC) is one of the most common cancers and one of the most common causes of cancer-related deaths worldwide (1). Although the survival rates of CRC patients have improved due to therapeutic advances, metastasis to other organs still hinders treatment success (2). Therefore, identifying the critical genes involved in the regulation of invasion and metastasis is important for improving cancer prognosis and treatment of CRC.

Peroxisome proliferator-activated receptor γ coactivator 1α (PGC-1α) is a nuclear receptor coactivator, which acts as a master regulator of mitochondrial biogenesis and cell metabolism (3). It was first noted to interact with peroxisome proliferator-activated receptor γ (PPARγ) in brown adipose tissue (4). Several studies have shown that PGC-1α expression is dysregulated in cancers and metastasis (5-9). For example, PGC-1α expression was shown to be reduced in colon (5), breast (6), and ovarian cancer (7). In contrast, PGC-1α expression is elevated in other cancers (8, 9). Correspondingly, its role and its underlying mechanism in cancer promotion is still controversial (10). Recently, we demonstrated that PGC-1α may be a poor prognostic indicator and be related to lymph node metastasis in CRC patients (11). It has been demonstrated that PGC-1α overexpression enhances cell proliferation and tumorigenesis of HEK293 cells *via* the up-regulation of Sp1 and acyl-CoA binding protein (ACBP) (12). We also, suggested that the expression of fatty acid synthase (FASN) is regulated by PGC-1α and may be contributing to increased cell proliferation (13). Although intensively studied, the role of PGC-1α in CRC invasion and metastasis is currently limited.

Wnt/β-catenin signaling is frequently activated in CRC and promotes the epithelial-mesenchymal transition (EMT) and metastasis (14, 15). EMT is related to invasion and metastasis (16). AKT is involved in the regulation of several cellular processes, such as cell survival, growth, migration, angiogenesis, and EMT, and is often found hyperactivated in many cancers (17, 18). Glycogen synthase kinase-3β (GSK-3β). is one of the downstream targets of AKT, which may be directly phosphorylated at Ser9 and be inactivated by p-AKT, potentially leading to β-catenin stabilization in the canonical Wnt signaling pathway.

Therefore, in this study, we aimed to explore the effect of knocking down PGC-1α in the CRC cell line SW620, which

Correspondence to: Joo-In Park, MD, Ph.D., Department of Biochemistry, Dong-A University College of Medicine, 32, Daesingongwon-ro, Seo-Gu, Busan 49201, Republic of Korea. Tel: 82 512402881, e-mail: jipark@dau.ac.kr

Key Words: Peroxisome proliferator activated receptor γ coactivator-1α (PGC-1α), colorectal cancer, AKT, glycogen synthase kinase-3β (GSK-3β), β-catenin.

highly expresses PGC-1α. In addition, we investigated the effect of PGC-1α overexpression in SW480 cells, another CRC cell line, which has low expression of PGC-1α. We examined cell proliferation, migration, and invasion and studied the underlying molecular mechanisms, with a focus on molecules such as p-AKT, GSK-3β, and β-catenin.

Materials and Methods

Cell cultures. Human CRC cell lines SW620 and SW480 were obtained from the Korean Cell Line Bank (Seoul National University, Seoul, Korea) and cultured in Dulbecco's modified Eagle's medium (DMEM) (Hyclone, Logan, UT, USA) supplemented with 10% fetal bovine serum (FBS)(Gibco, Carlsbad, CA, USA), 100 U/ml penicillin, and 100 μg/ml streptomycin (Hyclone, Pasching, Austria). Cultures were maintained in a humidified atmosphere of 95% air/5% CO_2 at 37˚C.

Materials. Crystal violet and agarose were obtained from Sigma-Aldrich (St. Louis, MO, USA). Antibodies against AKT (#4685), phospho-AKT (p-AKT; #4060), cyclin D1 (#2926), PTEN (#9556), GSK-3β (#9332), phospho-GSK-3β (p-GSK-3β; #9336), N-cadherin (#13116) and E-cadherin (#3195) were purchased from Cell Signaling Technology (Danvers, MA, USA). Anti-vimentin antibody (ab92547) was from Abcam (Cambridge, UK). Antibodies against phospho-β-catenin (p-β-catenin; sc-16743R) and β-catenin (sc-7199) were from Santa Cruz Biotechnology (Santa Cruz, CA, USA). Antibody against PGC-1α (ST1203) was from Merck Millipore (Burlington, MA, USA). The anti-β-actin (A1978), anti-rabbit IgG (A0545), and anti-mouse IgG secondary antibodies (A9044) were purchased from Sigma-Aldrich (St. Louis, MO, USA). Unless otherwise stated, all other chemicals were purchased from Sigma-Aldrich.

Generation of stable PGC-1α shRNA-knockdown SW620 cell line and PGC-1α overexpressing SW480 cell line. For the establishment of stable PGC-1α-knockdown, SW620 cells were transfected with 4 μg of nontargeting control (NC) shRNA or PGC-1α shRNA plasmid (catalog number 336313 KH00461N; Qiagen, Hilden, Germany) using Lipofectamine 2000 (Invitrogen, Carlsbad, CA, USA) following the manufacturer's instructions. After transfection, cells were treated with G418 (800 μg/ml) for 14 days and 6 clones were isolated. Among them, PGC-1α shRNA-1 and PGC-1α shRNA-6 SW620 cells were efficiently knocked-down and used in this study. For the establishment of a stable PGC-1α overexpressing SW480 line, the cells were transfected with 4 μg of empty vector (pcDNA3.1) or pcDNA3.1-FLAG-PGC-1α expression vector from Spiegelman using Lipofectamine 2000 (Invitrogen, Carlsbad, CA, USA) following the manufacturer's recommended procedure. After transfection, stable cell lines (PGC-1α-2- and PGC-1α-3-SW480 cells) were established after G418 selection (800 μg/ml) for 14 days.

Cell counting. Cells were cultured at a density of 1.5×10^5/well in 6-well plates. SW620, NC shRNA-, PGC-1α shRNA-1, PGC-1α shRNA-6 SW620 cells, SW480, pcDNA-, PGC-1α-2-, and PGC-1α-3-SW480 cells were cultured for 24, 48 and 72 h, respectively. A hemocytometer was used to count and calculate the average number of cells in each group. The experiments were repeated three times.

Cell proliferation assay. Cell proliferation was measured using the carboxyfluorescein succinimidyl ester (CFSE) labeling assay as previously described (12). Briefly, cells were washed three times with PBS and incubated with 1 μM CFSE dye (Molecular Probes) for 15 min. Then, the cells were washed again, incubated with fresh medium containing 10% FBS, and seeded in 6-well plates at a density of 1×10^5 cells/well. Cells were analyzed by flow cytometry (FACSCAlibur; BD Biosciences, San Jose, CA, USA) after culture for 24, 48, or 72 h. Experiments were performed three times.

Wound-healing assay. Cells were seeded on 6-well plates in DMEM containing 10% FBS. After 24 h, straight lines were drawn by scraping the confluent cells with a yellow tip. Then, the medium and floating cells were carefully removed, and the adherent cells were rinsed with normal saline three times and allowed to culture with serum-free DMEM. Following further incubation for the indicated times, the wound-healing process was monitored under a phase-contrast microscope, and representative images were acquired at 0, 24, 48, 72 and 96 h, respectively. The extent of cell migration is indicated as the percentage of scratch wound closure compared to the scratch at time zero. All experiments were performed three times.

Transwell migration and invasion assays. Transwell migration assays were performed using 24-well cell culture plate transwell inserts (353097; Corning Inc., Lowell, MA, USA) with 8 μm pore filters. Cells (1×10^5) in serum-free medium were seeded into the upper chamber of the insert and complete medium was added to the lower chamber. After incubation for 48 h, the cells on the upper surface were removed using cotton tips and the cells that migrated to the underside of the membrane were fixed with 4% formaldehyde in PBS for 30 min at RT, stained with 0.1% crystal violet (Sigma Aldrich, St. Louis, MO, USA) for 20 min and washed with PBS three times. The number of cells was calculated from five random fields at a magnification of ×200, using an inverted microscope (Nikon Eclipse TS100; Nikon, Tokyo, Japan) and expressed as the average number of cells/field of view. The mean value was calculated from three independent experiments. For transwell invasion assays, cells (1×10^5) were suspended in 200 μl of serum free medium and inoculated into upper chambers of 24-well cell culture plate transwell inserts (353097; Corning Inc., Lowell, MA, USA) that were precoated with 50 μl of 1 μg/μl Matrigel (BD Biosciences, San Jose, CA, USA). The lower compartment of each chamber had 600 μl DMEM with 10% FBS added and the plate incubated for 48 h at 37˚C with 5% CO_2. Then, the cells on the upper surface were removed using cotton tips and the cells that migrated to the underside of the membrane were fixed with 4% formaldehyde in PBS for 30 min at RT, stained with 0.1% crystal violet (Sigma Aldrich, St. Louis, MO, USA) for 20 min and washed with PBS three times. The number of cells was calculated from five random fields at a magnification of ×200, using an inverted microscope (Nikon Eclipse TS100; Nikon, Tokyo, Japan) and expressed as the average number of cells/field of view. The mean value was calculated from three independent experiments.

Western blot analysis. Cell lysis and western blot analyses were performed as described previously (19). In brief, cells were treated with lysis buffer (20 mM Tris, pH 8.0, 137 mM NaCl, 10% glycerol, 1% Nonidet P-40, 10 mM EDTA, 100 mM NaF, 1 mM phenylmethylsulfonyl fluoride, and 10 mg/ml leupeptin). The

lysates were centrifuged at 13,000 rpm for 15 min, and the concentration of protein in each lysate was determined by Bio-Rad protein assay (Bio-Rad Lab., Richmond, CA, USA), according to the manufacturer's suggested procedure. The lysates (30 μg protein) were separated with SDS-PAGE and then transferred to PVDF membranes (Merck Millipore, Darmstadt, Germany). Blots were blocked for 1 h in 5% skim milk in PBS at room temperature (RT). Then, blots were probed with the appropriate primary antibody overnight at 4˚C. After washing, blots were probed with horseradish peroxidase-conjugated secondary antibodies for 2 h. After another wash, the signals were detected with ECL (Amersham, Buckinghamshire, UK) according to the manufacturer's instructions. The blots were also probed with a monoclonal anti-β-actin antibody, which served as an internal loading control. Bands were quantified using Image Studio Lite Ver 3.1. (LI-COR, Inc., Lincoln, NE, USA).

Immunofluorescence staining. Cells were cultured on a Lab-Tek® Chamber Slide™ (Nalge Nunc, Inc., Rochester, NY, USA) and then fixed with 3% formaldehyde, permeabilized using 0.3% Triton X-100, and blocked for 30 min with 5% bovine serum albumin (BSA) at RT. Next, the cells were washed, and a series of antibodies was used as indicated, followed by staining with FITC-conjugated goat anti-mouse IgG (Santa Cruz Biotechnology, Santa Cruz, CA, USA) or Cy3-conjugated donkey anti-rabbit IgG (Invitrogen, USA, Merck Millipore, USA). The samples were then mounted using glycerol, and analyzed by confocal microscope (Carl Zeiss LSM800; Carl Zeiss, Jena, Germany) with a 40× C-Apochromat objective. Negative control staining was performed using only secondary antibodies. Nuclei were stained with Hoechst.

Myr-Akt expression vector transfection. PGC-1α shRNA-SW620 cells were transfected with 4 μg of myc-tagged myristoylated AKT expression vector (Myr-AKT) or empty vector (pUSEamp, Upstate Technology) using lipofectamine 2000 according to the manufacturer's instruction. After transfection, cells were cultured in 10% FBS-supplemented DMEM for 48 h. These cells were then used for cell proliferation, transwell invasion assay and western blot analysis.

Immunoprecipitation. Cells (NC shRNA-, PGC-1α shRNA-SW620, pcDNA-, and PGC-1α-SW480 cells) were lysed in 500 μl of RIPA lysis buffer (150 mM NaCl, 10 mM Tris-HCl, pH 7.2, 0.1% SDS, 1% Triton X-100, 5 mM EDTA, 1X protease inhibitor, 1 mM PMSF, 100 μM Na_3VO_4, and phosphatase inhibitor cocktail). The supernatants were collected by centrifugation at 13,000 rpm for 10 min at 4˚C, and the protein concentration was determined by Bradford assay (Bio-Rad, Hercules, CA). For immunoprecipitaion, 0.8 mg of protein diluted in lysis buffer was incubated with a PGC-1α antibody (1:100) or AKT antibody (1:100) for 1 h at 4˚C. The immune complexes were captured with Recombinant Protein G Agarose (Invitrogen, Carlsbad, CA, USA) overnight with rotation. Immunoprecipitates were subjected to SDS-PAGE and western blot analysis using an antibody to PGC-1α or AKT.

Statistical analysis. Statistical analyses were performed with the SPSS 23.0 statistical package for Windows (SPSS, Chicago, IL, USA). Data are expressed as the mean±standard deviation (SD). One-way analysis of variance (ANOVA) and unpaired Student's t test were used to determine statistical significance. Statistical significance was defined as $p<0.05$.

Results

PGC-1α knockdown suppresses cell proliferation. SW620 and SW480 cells are isogenic cell lines derived from the same patient and their invasion ability differs (20). First, we examined the expression level of PGC-1α in SW480 and SW620 cells. As expected, the expression level of PGC-1α in SW620 cells was higher than that in SW480 cells (0.2±0.0-fold, $p<0.001$ compared to SW620 cells; Figure 1A). To evaluate the function of PGC-1α in the high-expressing CRC cell line, it was knocked down by stable transfection with a short hairpin RNA (PGC-1α shRNA) plasmid. PGC-1α expression was reduced by more than 80% in PGC-1α knockdown cells (PGC-1α shRNA-1 and -6 SW620 cells; 23±5%, $p<0.001$ and 16±2%, $p<0.001$, respectively) compared to control cells transfected with a nontargeting control shRNA sequence (NC shRNA-SW620 cells) (Figures 1B and C). To investigate whether PGC-1α can modulate cell proliferation, we first examined the effect of its knockdown on the cell growth of SW620 cells. Control, NC shRNA-, PGC-1α shRNA-1, or -6 SW620 cells were cultured for 24, 48, or 72 h and cell proliferation was measured by cell counting and CFSE labeling assays. Cell proliferation of PGC-1α shRNA-1 (cell counts: 1.9±0.1 at 24 h, $p<0.05$; 5.1±0.2 at 48 h, $p<0.001$; 13.8±1.0 at 72 h, $p<0.001$) and -6 SW620 cells (cell counts: 1.9±0.1 at 24 h, $p<0.05$; 4.4±0.1 at 48 h, $p<0.001$; 12.1±0.7, $p<0.001$) was significantly inhibited at all time points, compared to SW620 (cell counts: 2.5±0.1 at 24 h; 7.5±0.3 at 48 h; 18.6±0.4 at 72 h) and NC shRNA SW620 cells (cell counts: 2.6±0.3 at 24 h; 7.4±0.3 at 48 h; 18.9±0.3 at 72 h) (Figure 1D). CFSE labeling assay confirmed that PGC-1α knockdown decreased cell proliferation in SW620 cells (% of proliferating cells in PGC-1α shRNA-1 and -6 cells: 3.2±0.7, $p<0.001$ at 72 h and 2.1±0.5, $p<0.001$ at 72 h *vs*. 42.1±3.1 and 42.0±2.3 at 72 h in control and NC shRNA-SW620 cells; Figure 1E). The results clearly demonstrate that loss of PGC-1α expression inhibits cell proliferation of SW620 cells.

PGC-1α knockdown inhibits cell migration and invasion. We evaluated the migration and invasion ability of PGC-1α shRNA-SW620 cells using wound-healing, transwell migration and invasion assays. Wound closure was significantly inhibited in the PGC-1α shRNA-1 and -6 SW620 cells (48.2±0.7% at 96 h, $p<0.001$ and 45.2 ±5.7% at 96 h, $p<0.001$, respectively) compared to the SW620 and NC shRNA-SW620 cells (84.2±9.5 at 96 h and 78.5±7.4 at 96 h, respectively; Figure 2A). In addition, transwell migration assay results showed that the number of trans-membrane migrated cells was significantly lower in the PGC-1α shRNA-1 and -6 SW620 cells (95.8±10.8, $p<0.001$ and 86.4±6.9, $p<0.001$, respectively) compared to SW620 and NC shRNA-SW620 cells (205.6±14.7 and

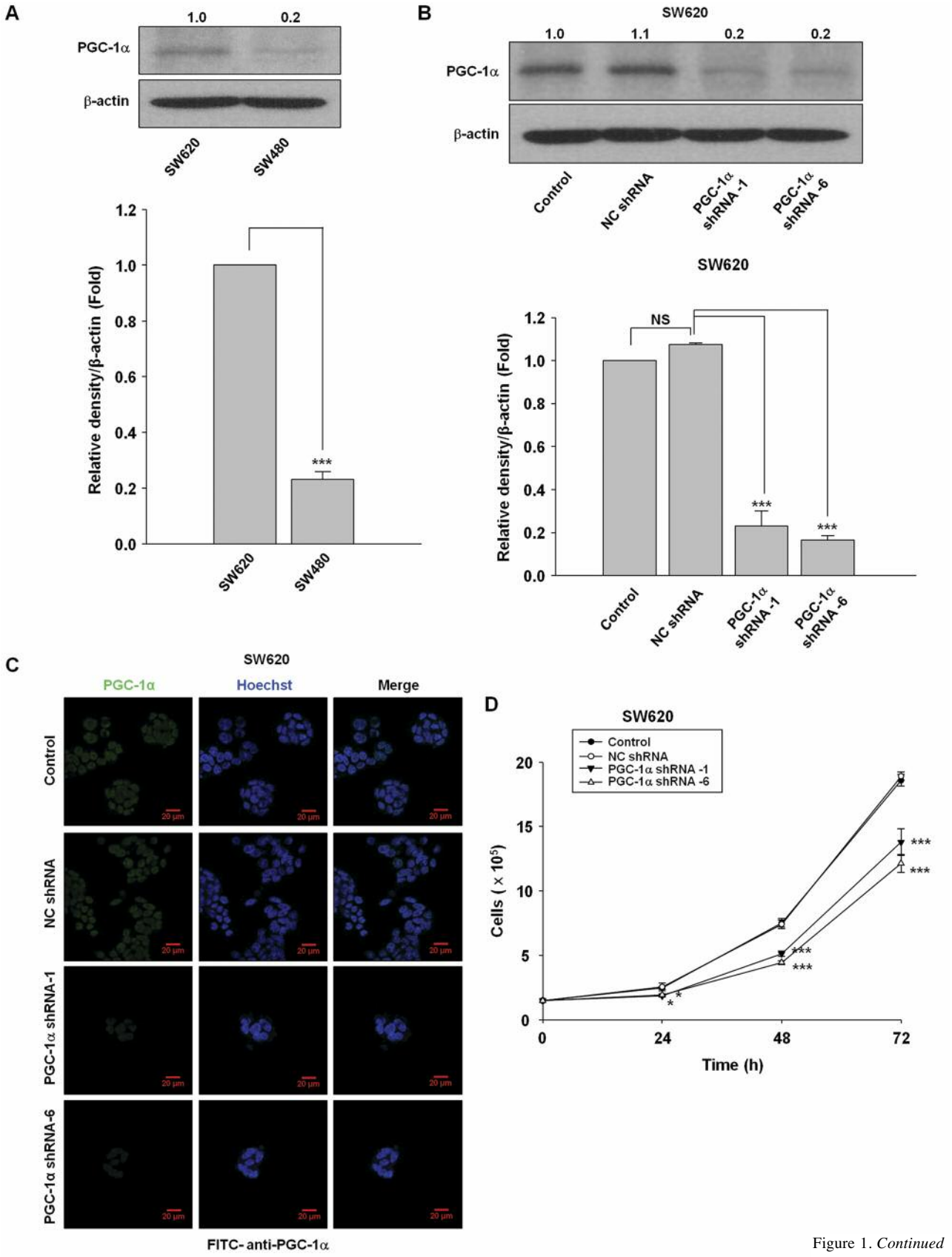

Figure 1. *Continued*

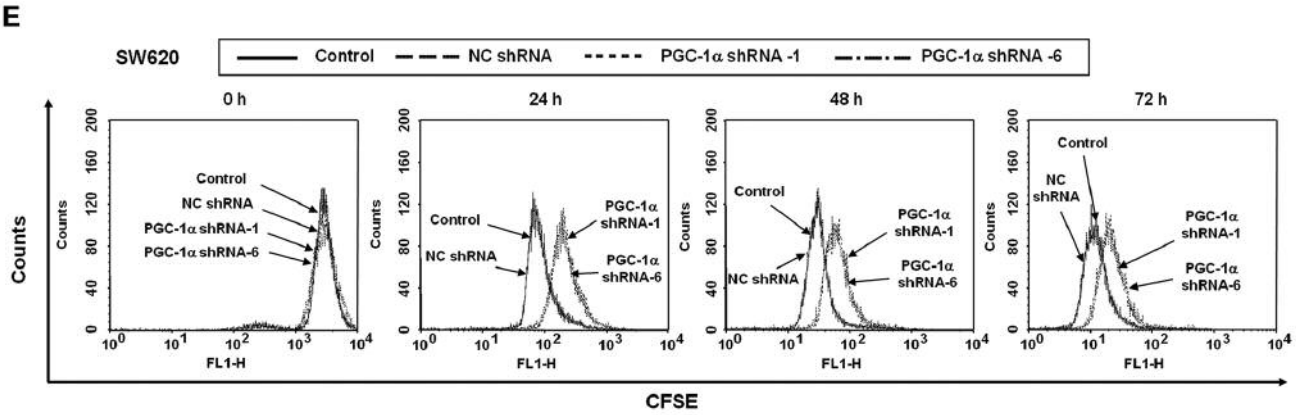

Figure 1. *PGC-1α knockdown inhibits cell proliferation. (A and B) PGC-1α expression was examined by western blot analysis with an anti-PGC-1α antibody. β-actin was used as an internal control. Representative densitometry results are indicated above the bands. (A) Upper panel: PGC-1α expression in SW620 and SW480 cells. Lower panel: Relative protein level compared with β-actin by densitometry was expressed as mean±SD (n=3). ***p<0.001 vs. SW620 cells. (B) Upper panel: SW620 cells were transfected with PGC-1α shRNA or nontargeting control (NC) shRNA and screened based on the resistance to G418 (800 μg/ml). PGC-1α expression was detected by western blot analysis. Representative densitometry results are indicated above the bands. Lower panel: Relative protein level compared with β-actin by densitometry was expressed as mean±SD (n=3). ***p<0.001 vs. control or NC shRNA. NS indicates no significance. (C) PGC-1α expression was observed under a confocal microscope by immunofluorescence staining with FITC-labelled PGC-1α antibody. Cells were co-labelled with Hoechst. The results are representative of three independent experiments. (D and E) Control, NC shRNA-, PGC-1α shRNA-1, or -6 SW620 cells were seeded and cultured for the indicated times and cell proliferation was determined by cell counting (D). The data represent the mean±SD of three separate experiments. *p<0.05, ***p<0.001, vs. control or NC shRNA-SW620 cells. (E) CFSE staining. CFSE labelled control, NC shRNA-, PGC-1α shRNA-1, or -6 SW620 cells (1×10^5 cells/well) were incubated with fresh medium containing 10% FBS for the indicated times. The samples were analysed by flow cytometry using a FACScan flow cytometer. Data analysis was performed using CellQuest software (BD Biosciences).*

199.4±15.1, respectively; Figure 2B). Transwell invasion assay results showed that the number of cells that passed through the Matrigel was significantly lower in the PGC-1α shRNA-1 and -6 SW620 cells (44.2±13.4, $p<0.01$ and 28.2±4.7, $p<0.001$, respectively) compared to SW620 and NC shRNA-SW620 cells (161.4±52.3 and 127.8±21.0, respectively; Figure 2C). Collectively, these data indicate that PGC-1α knockdown inhibits cell migration and invasion.

PGC-1α knockdown reduces the expression of β-catenin, GSK-3β and EMT-associated genes as well as AKT phosphorylation. Based on the observations described above, we invesigated whether PGC-1α affects EMT. EMT is known to be an important regulator in cell migration and invasion (16). Morphologically, NC shRNA-SW620 cells were spindle, mesenchymal cell-like, but PGC-1α shRNA-SW620 cells were round and epithelial cell-like. NC shRNA-SW620 cells expressed higher levels of the mesenchymal cell marker, vimentin, compared to PGC-1α shRNA-SW620 cells (Figure 3A). Western blot analysis showed that PGC-1α knockdown (PGC-1α shRNA-1 and -6 SW620 cells) reduced the expression of N-cadherin (0.1- and 0.1-fold) and vimentin (0.3- and 0.5-fold), however the expression of E-cadherin was increased compared to the control NC shRNA SW620 cells (3.7- and 3.9-fold, Figure 3B). Wnt/β-catenin signaling is known to be involved in the regulation of EMT and invasion, therefore, we examined whether PGC-1α can regulate Wnt/β-catenin signaling. Western blot analyses showed that PGC-1α knockdown significantly decreased β-catenin (0.2- and 0.2-fold) as well as β-catenin signaling targets, including c-Myc (0.1- and 0.0-fold) and cyclin D1 (0.4- and 0.4-fold), which was accompanied by increased β-catenin phosphorylation (Ser33/37/Thr141)(6.2- and 6.0-fold) in SW620 cells (Figure 3B). To further investigate the mechanism of inhibition of β-catenin signaling by PGC-1α knockdown, we investigated the status of GSK-3β, a negative regulator of β-catenin signaling and a downstream target of AKT. Our results showed that PGC-1α knockdown significantly down-regulated AKT phosphorylation at Ser473 (active AKT) (0.1- and 0.1-fold) and GSK-3β phosphorylation at the Ser9 site (inactive GSK-3β) (0.1- and 0.2-fold; Figure 3B). In addition, total AKT (0.4- and 0.4-fold) and GSK-3β expression (0.2- and 0.3-fold) was also down-regulated by PGC-1α suppression (Figure 3B). These findings suggest that PGC-1α knockdown inhibits AKT activity and expression, and further, increases GSK-3β activity as a result of the decrement in GSK-3β phosphorylation at Ser9.

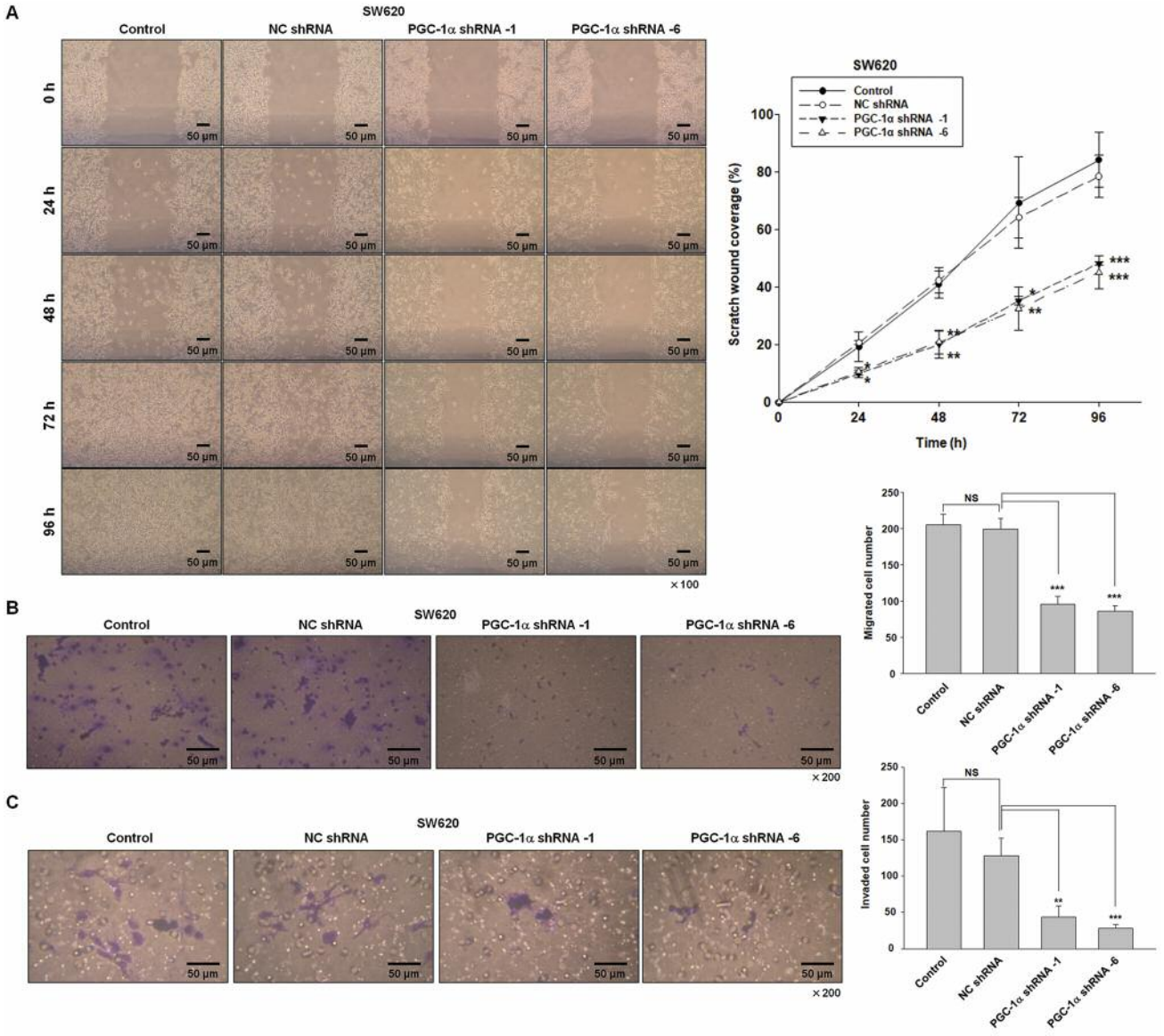

Figure 2. *PGC-1α knockdown inhibits migration and cell invasion. (A) Left panel: Wound-healing assay (magnification, ×100). Right panel: The extent of cell migration is indicated as the percentage of scratch wound closure compared to the scratch area at time point 0 h. Data are expressed as the mean±SD of three independent experiments. *p<0.05, **p<0.01, ***p<0.001 vs. NC shRNA SW620 cells. (B) Left panel: Transwell migration assay was performed in control, NC shRNA-, PGC-1α shRNA-1, or -6 SW620 cells. Representative figures of control, NC shRNA-, PGC-1α shRNA-1, or -6 SW620 cells in the transwell migration assay (×200 magnification). Right panel: The number of migrated cells was counted on five randomly chosen visual fields. Data are expressed as the mean±SD of three independent experiments. ***p<0.001 vs. NC shRNA SW620 cells. NS indicates no significance. (C) Left panel: Transwell invasion assay was performed in control, NC shRNA-, PGC-1α shRNA-1, or -6 SW620 cells. Representative figures of control, NC shRNA-, PGC-1α shRNA-1, or -6 SW620 cells in the transwell invasion assay (×200 magnification). Right panel: The numbers of invaded cells were counted under five randomly chosen visual fields. Data are expressed as the mean±SD of three independent experiments. **p<0.01, ***p<0.001 vs. NC shRNA SW620 cells. NS indicates no significance.*

To determine whether PGC-1α knockdown inhibits cell growth, migration, invasion, and β-catenin activation specifically through the inhibition of AKT/GSK-3β signaling, we transfected the constitutively active AKT-expression vector (Myr-AKT) into PGC-1α shRNA-SW620 cells and examined cell proliferation, migration, and invasion. Myr-Akt reversed the inhibition of GSK-3β (0.9-fold) and β-catenin (1.2-fold) by PGC-1α knockdown (Figure 3C), along with cell proliferation (1.3-fold at 24 h, $p<0.01$; 1.2-fold at 48 h, $p<0.01$; 1.3-fold at 72 h, $p<0.001$; Figure 3D) and invasion

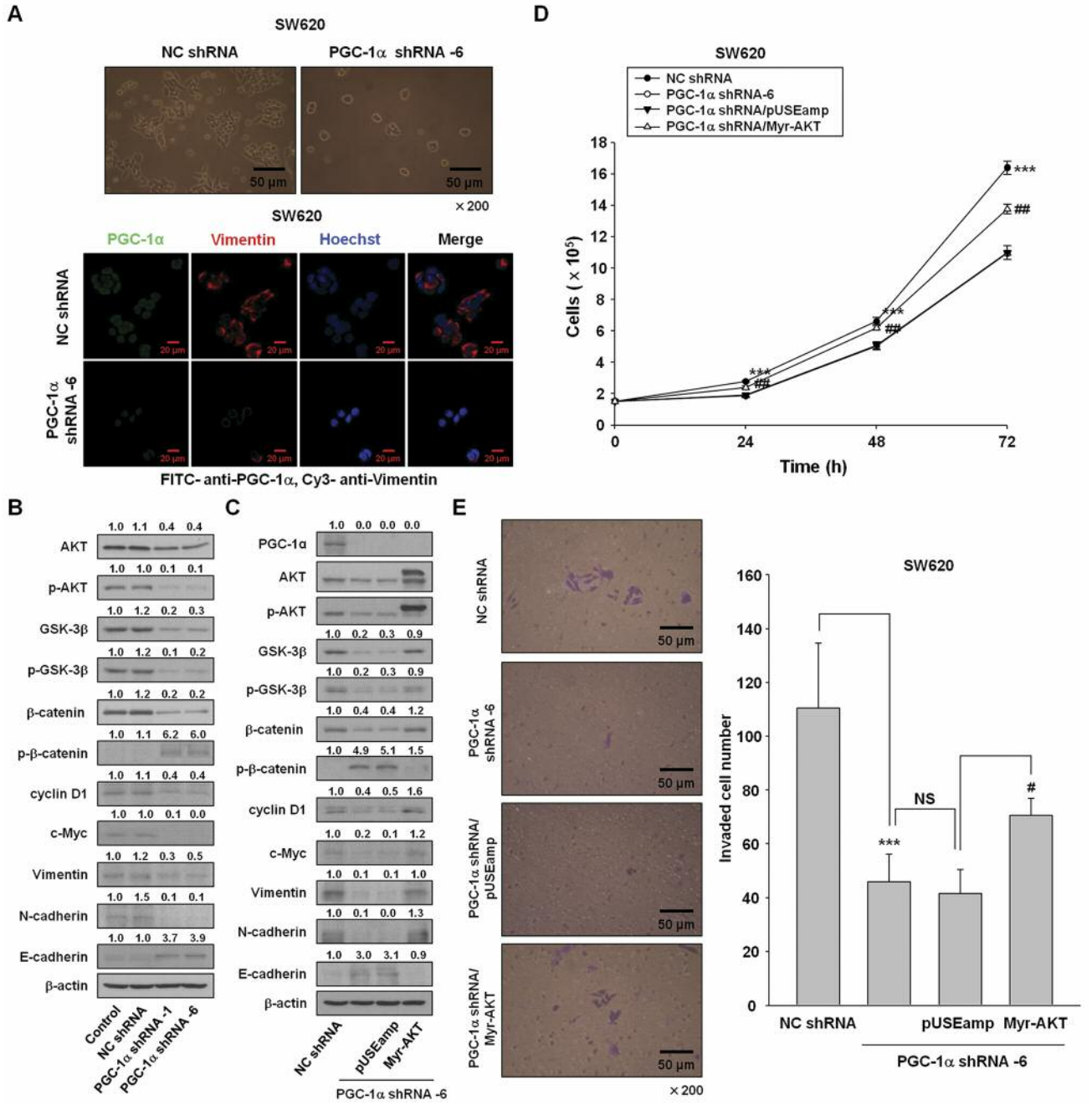

Figure 3. *PGC-1α knockdown reduces the expression of p-AKT, p-GSK-3β, and β-catenin, and constitutively active AKT (Myr-AKT) transfection reverses the PGC-1α knockdown-induced inhibition of cell proliferation and invasion in SW620 cells. (A) Upper panel: Morphological observation shows that NC shRNA-SW620 cells have a mesenchymal-like spindle shape, but PGC-1α shRNA-SW620 cells have an epithelial morphology. Lower panel: Immunofluorescence staining was performed to detect PGC-1α (FITC) and mesenchymal cell marker (vimentin; Cy-3) in NC shRNA-SW620 and PGC-1α shRNA-SW620 cells. Nuclei were stained with Hoechst. (B) Western blot was used to detect the expression of the key signaling molecules. β actin was used as an internal control. Densitometry results are expressed above the bands. Representative data of three independent experiments. Relative protein expression of each protein was quantified using Image Studio Lite Ver 3.1 and normalized to β-actin. (C) PGC-1α shRNA-SW620 cells were transiently transfected by lipofetamine 2000 for 48 h with pUSEamp vector or Myr-AKT expression vector, respectively. After transfection, protein lysates were prepared and used for western blot analysis with the corresponding antibodies. β-actin was used as a loading control. The blot is representative of three separate experiments. Densitometry results are expressed above the bands. (D) Myr-AKT transfection recovered cell proliferation in PGC-1α shRNA-SW620 cells. ***p<0.001 vs. PGC-1α shRNA-SW620 cells. ##p<0.01 vs. PGC-1α shRNA/pUSEamp-SW620 cells. (E) Constitutively active AKT reverses the diminished cell invasion by PGC-1α knockdown. ***p<0.001 vs. NCshRNA-SW620 cells; #p<0.05 vs. PGC-1α shRNA/pUSEamp-SW620 cells. NS indicates no significance.*

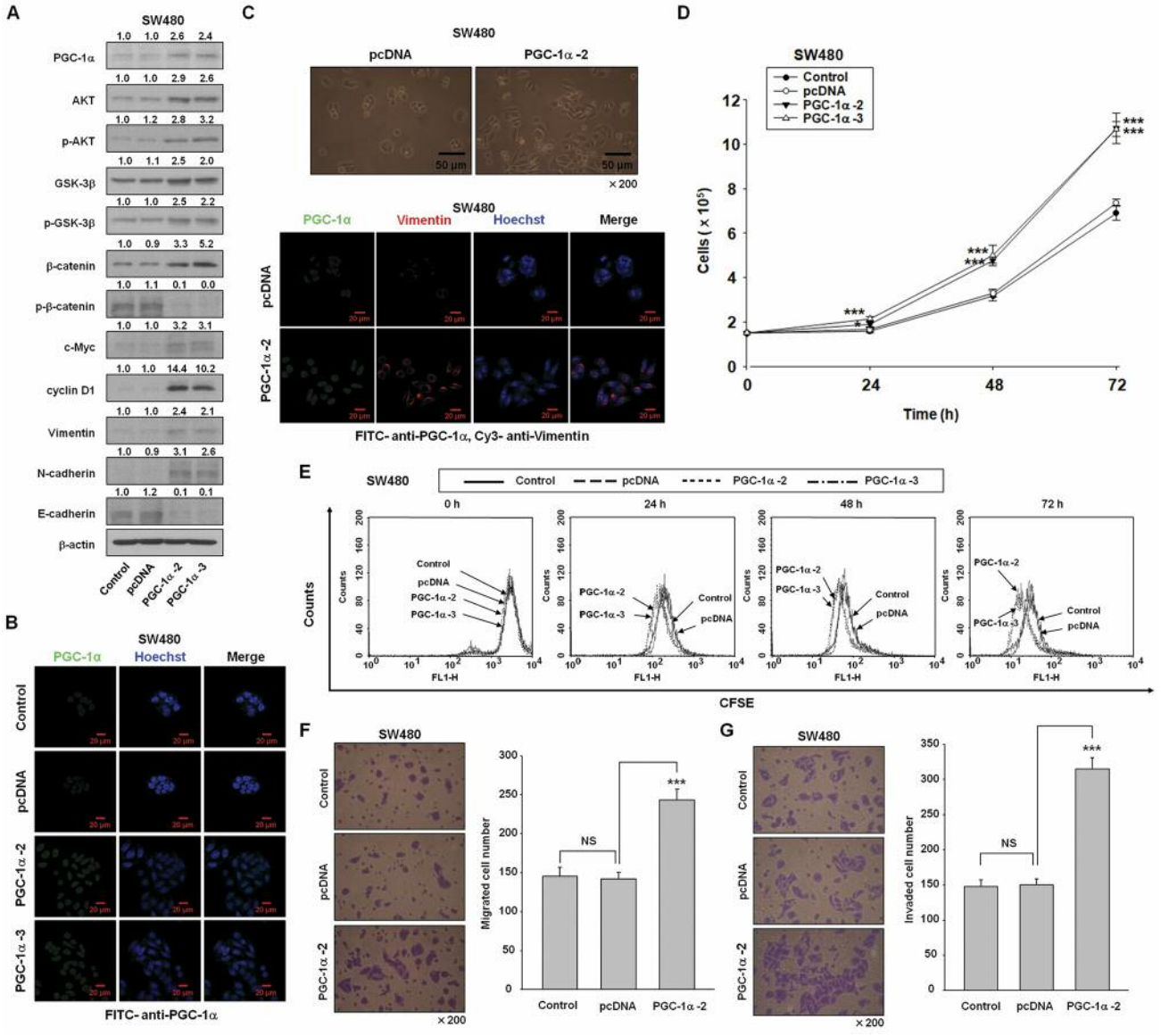

Figure 4. *PGC-1α overexpression enhances cell proliferation and invasion in SW480 cells. (A) SW480 cells were transfected with PGC-1α or pcDNA3.1 expression vector and screened based on the resistance to G418 (800 μg/ml). Western blot was used to detect PGC-1α and the key signaling molecules. β-actin was used as an internal control. Densitometry results are indicated above the bands. Representative data of three independent experiments. (B) PGC-1α expression was observed under a confocal microscope by immunofluorescence staining with FITC-labelled PGC-1α antibody. Cells were co-labelled with Hoechst. The results are representative of three independent experiments. (C) Upper panel: Morphological observation showed that PGC-1α-2 SW480 cells have a mesenchymal-like spindle shape, but pcDNA-SW480 cells have an epithelial morphology. Lower panel: Immunofluorescence staining was performed to detect PGC-1α (FITC) and mesenchymal cell marker (vimentin; Cy-3) in pcDNA-SW480 and PGC-1α-SW480 cells. Nuclei were stained with Hoechst. (D and E) Control, pcDNA-, PGC-1α-2, or -3 SW480 cells were seeded and cultured for the indicated times and cell proliferation was determined by cell counting (D). The data represent the mean±SD of three separate experiments. *p<0.05, ***p<0.001, vs. Control or pcDNA-SW480 cells. (E) CFSE staining. CFSE labelled control, pcDNA-, PGC-1α-2, or -3 SW480 cells (1×10^5 cells/well) were incubated with fresh medium containing 10% FBS for the indicated times. The samples were analysed by flow cytometry using a FACScan flow cytometer. Data analysis was performed using CellQuest software (BD Biosciences). (F) Left panel: Transwell migration assays were performed in control, pcDNA-, and PGC-1α-2 SW480 cells. Representative figures of control, pcDNA-, PGC-1α-2 SW480 cells in the transwell migration assay are shown (×200 magnification). Right panel: The number of trans-membrane migrated cells was counted on five randomly chosen visual fields. Data are expressed as the mean±SD of three independent experiments. ***p<0.001 vs. Control or pcDNA-SW480 cells. NS indicates no significance. (G) Left panel: Transwell invasion assay was performed in control, pcDNA-, PGC-1α-2 SW480 cells. Representative figures of control, pcDNA-, PGC-1α-2 SW480 cells in the transwell invasion assay (×200 magnification). Right panel: The numbers of invaded cells were counted under five randomly chosen visual fields. Data were expressed as the mean±SD of three independent experiments. ***p<0.001 vs. Control or pcDNA-SW480 cells. NS indicates no significance.*

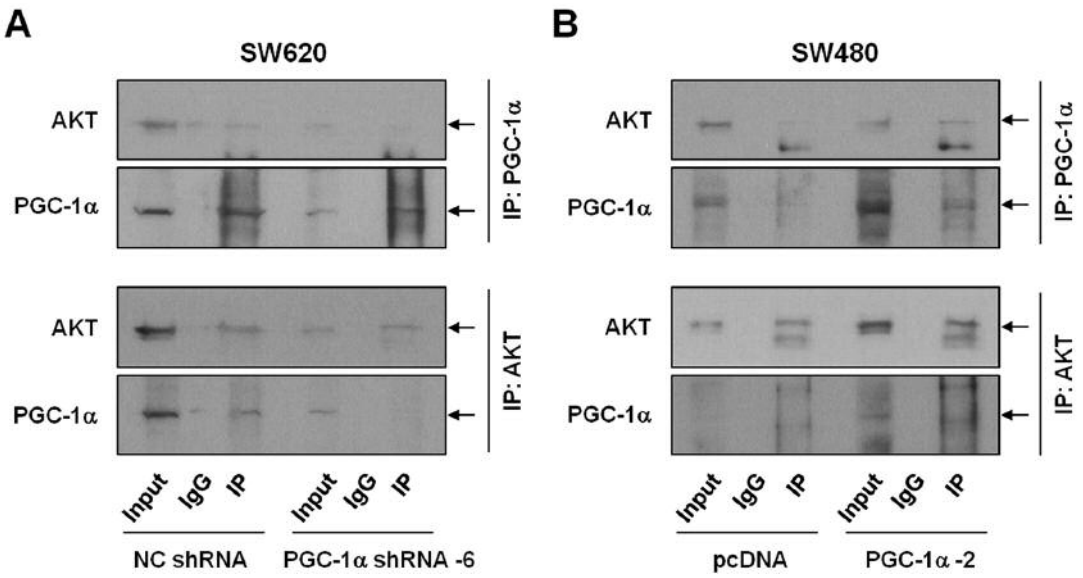

Figure 5. *Direct interaction of PGC-1α and AKT in SW620 and SW480 cells. (A) NC shRNA-SW620 and PGC-1α shRNA-6 SW620 cells were lysed in RIPA buffer. PGC-1α proteins (upper) and AKT proteins (lower) were co-immunoprecipitated by incubating the cell lysates with PGC-1α antibody or AKT antibody, followed by recombinant protein G agarose with anti-mouse IgG or anti-rabbit IgG, respectively. Immunoprecipitated proteins were solubilized in SDS sample buffer and separated by SDS-PAGE. Blots were probed with anti-PGC-1α or anti-AKT antibodies. (B) pcDNA-SW480 and PGC-1α-SW620 cells were lysed in RIPA buffer. PGC-1α proteins (upper) and AKT proteins (lower) were immunoprecipitated by incubating the cell lysates with PGC-1α antibody or AKT antibody, followed by recombinant protein G agarose with anti-mouse IgG or anti-rabbit IgG, respectively. Immunoprecipitated proteins were solubilized in SDS sample buffer and separated by SDS-PAGE. Blots were probed with anti-PGC-1α or anti-AKT antibodies. IP: Immunoprecipitation.*

(cell numbers being; 70.6±6.3 *vs*. 41.6±8.8, $p<0.05$; Figure 3E) in SW620 cells. Taken together, our data suggest that PGC-1α knockdown inhibits cell proliferation, invasion and β-catenin signaling, by inhibition of the AKT/GSK-3β axis.

PGC-1α overexpression enhances cell proliferation and invasion. Since knockdown of PGC-1α inhibits the proliferation and invasion of SW620 cells, we speculated that overexpression of PGC-1α might exert a stimulatory effect on cell proliferation and invasion. To test our hypothesis, we tranfected SW480 cells, which have low endogenous levels of PGC-1α, with the PGC-1α expression vector to establish PGC-1α overexpressing SW480 cells (PGC-1α-2, or -3 SW480 cells). We confirmed the increased expression of PGC-1α (2.6-fold and 2.4-fold) by western blot analysis and immunofluorescence staining (Figures 4A and B). Morphological observation showed that PGC-1α-SW480 cells seem to be mesenchymal-like, but pcDNA-SW480 cells looked epithelial (Figure 4C). In addition, PGC-1α-SW480 cells expressed higher levels of vimentin compared to pcDNA-SW480 cells (Figure 4C). Cell counting showed that cell proliferation of PGC-1α-2 and -3 SW480 cells (cell counts: 1.9±0.1, $p<0.05$ and 2.1±0.1, $p<0.001$ at 24 h; 4.8±0.2, $p<0.001$ and 5.0±0.5, $p<0.001$ at

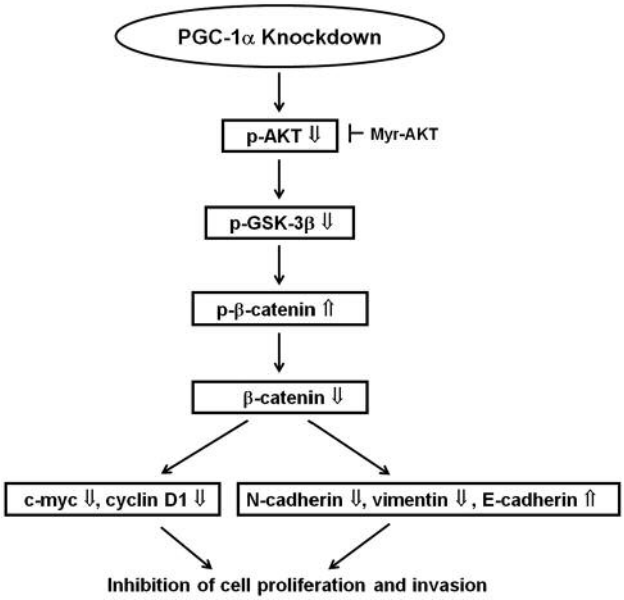

Figure 6. *The potential molecular mechanism by which PGC-1α knockdown inhibits cell proliferation and invasion in SW620 cells. In summary, PGC-1α knockdown inhibits cell proliferation and invasion via the inhibition of p-AKT/GSK-3β/β-catenin axis, resulting in suppressed expression of c-Myc, cyclin D1, N-cadherin, and vimentin, and increased expression of E-cadherin.*

48 h; 10.7±0.7, $p<0.001$ and 10.7±0.3, $p<0.001$ at 72, respectively) was increased, compared to that of control (1.6±0.1 at 24 h; 3.2±0.2 at 48 h; 6.9±0.3 at 72 h) or pcDNA-SW480 cells (1.7±0.1 at 24 h; 3.3±0.2 at 48 h; 7.4±0.2 at 72 h; Figure 4D). In addition, CFSE analysis showed that percentage of proliferating cells in PGC-1α-2 and -3 SW480 cells (79.0±1.9%, $p<0.001$ at 72 h and 79.9±1.3%, $p<0.001$ at 72 h) were significantly increased compared to that of the control (44.5±4.0% at 72 h) or pcDNA-SW480 cells (45.8±3.6% at 72 h) (Figure 4E). Transwell migration assay results demonstrated that the number of migrated PGC-1α-SW480 cells were higher compared to pcDNA-SW480 cells (243.0±14.1 *vs.* 142.2±8.3, $p<0.001$; Figure 4F). In addition, transwell invasion assay results showed that the number of cells that passed through the Matrigel was significantly higher in the PGC-1α-SW480 cells compared to pcDNA-SW480 cells (315.2±16.9 *vs.* 150.2±8.9, $p<0.001$; Figure 4G). Taken together, PGC-1α overexpression significantly enhanced cell proliferation and invasion. We also investigated the expression of p-AKT, p-GSK-3β, β-catenin, and EMT related proteins in PGC-1α-SW480 cells by western blot analysis. Western blot results showed that p-AKT (2.8-fold and 3.2-fold), p-GSK-3β (2.5-fold and 2.2-fold), β-catenin (3.3-fold and 5.2-fold), vimentin (2.4-fold and 2.1-fold) and N-cadherin (3.1-fold and 2.6-fold) were all increased, however, E-cadherin (0.1-fold and 0.1-fold) was inhibited in PGC-1α-2 and -3 SW480 cells, respectively (Figure 4A). These results are diametrically opposite to those seen with PGC-1α shRNA-SW620 cells.

Direct interaction of PGC-1α and AKT may contribute to the regulation of AKT signaling. Thus far, the findings suggest that PGC-1α regulates AKT activity. However, the underlying molecular mechanisms are not clearly defined. Therefore, we investigated whether PGC-1α physically interacts with AKT by performing co-immunoprecipitation. In PGC-1α immunoprecipitates (upper panel), the reaction with the AKT antibody showed that PGC-1α more strongly interacted with AKT in NC shRNA-SW620 and PGC-1α-2 SW480 cells compared to PGC-1α shRNA-6 SW620 and pcDNA-SW480 cells, respectively (Figure 5A and B). In addition, in AKT immunoprecipitates (lower panel), the reaction with the PGC-1α antibody showed that AKT more strongly interacted with PGC-1α in NC shRNA-SW620 and PGC-1α-2 SW480 cells compared to PGC-1α shRNA-6 SW620 and pcDNA-SW480 cells, respectively. These data suggest that a direct physical interaction between PGC-1α and AKT may contribute to the regulation of the AKT pathway, although the underlying mechanisms are undefined. Further studies are required to understand in more detail the molecular interaction of PGC-1α with AKT.

Discussion

The role of PGC-1α in cancer is still not unequivocal since both tumor suppressive and tumor promoting effects have been reported (10, 21). Its biological effects and underlying mechanisms are highly complex depending on the cancer cell type, its posttranslational modifications, and the functional status of its interacting proteins (10, 21). We have previously demonstrated, in a retrospective study, that PGC-1α might be an indicator of poor prognosis, as it is associated with lymph node metastasis in CRC patients (11). Several studies aimed at exploring the underlying mechanisms by which PGC-1α affects cell proliferation and tumorigenesis in CRC have been performed, and provided the following insights. PGC-1α was first reported to enhance cell proliferation and tumorigenesis through an up-regulation of Sp1 and ACBP (12). PGC-1α was also shown to increase cell proliferation by modulating FASN expression through the Sp1 and sterol responsive element binding protein-1c (SREBP-1c) (13). However, the molecular mechanisms by which PGC-1α affects cell invasion and metastasis in CRC are not clearly defined. Here, we established stable cell lines in which PGC-1α was knocked-down and found that PGC-1α shRNA-SW620 cells exhibited reduced cell proliferation, compared to control and NC shRNA-SW620 cells. These results are consistent with our previous observations (12, 13), although different cell lines were used. Taken together, these data demonstrate that PGC-1α can enhance cell proliferation in various cell lines, including HEK293 cells.

As described above, Wnt/β-catenin signaling is involved in CRC malignant progression as exhibited by invasion and metastasis (14, 15). Accumulating evidence suggests that EMT is an important process related to the invasion and metastasis (16), and is regulated by AKT (17, 18). GSK-3β is one of the downstream targets of AKT; it is inactivated by p-AKT, which causes β-catenin stabilization in the canonical Wnt signaling pathway. In this study, we observed that PGC-1α knockdown significantly inhibits cell migration and invasion. These results are consistent with Wang's study (22), showing that PGC-1α knockdown inhibits tumor growth and metastasis in gastric cancer. We investigated the expression of EMT related molecules in PGC-1α shRNA-SW620 cells. As expected, the results showed that the expression of N-cadherin and vimentin (mesenchymal markers) were decreased, whereas expression of E-cadherin (epithelial marker) was increased. In contrast to our results, LeBleu *et al*. demonstrated that PGC-1α enhances metastasis through enhancing mitochondrial biogenesis and oxidative phosphorylation in breast cancer, without affecting proliferation and the expression of EMT (23). In addition, Andrzejewski *et al*. revealed that PGC-1α promotes lung metastasis of breast cancer through the enhancement of global bioenergetic capacity (24). Because we were focused on understanding the effect of PGC-1α on the expression of

signaling molecules involved in cell proliferation and invasion, we did not examine the bioenergetic capacity in our cell lines. However, further studies to investigate this in NC shRNA- and PGC-1α shRNA-SW620 cells will be helpful to understand more accurately the role of PGC-1α in CRC. Taken together, these results indicate that the effect of PGC-1α on the expression of EMT related molecules is complicated and depends on the cancer cell type.

Since AKT is known to regulate EMT (17, 18), we hypothesized that the effects of PGC-1α on invasion and metastasis might be attributed to the regulation of AKT/GSK-3β/β-catenin axis. Interestingly, the results showed that p-AKT, p-GSK-3β, and β-catenin expression is significantly decreased in PGC-1α shRNA-SW620 cells, compared to NC shRNA-SW620 cells. Of particular importance in the light of these results, was that Myr-AKT transfection performed in PGC-1α shRNA-SW620 cells, to investigate whether down-regulation of p-AKT is required for growth and invasion inhibition, showed that Myr-AKT significantly reversed these effects by PGC-1α knockdown, strongly suggesting that down-regulation of p-AKT is required for the inhibition of cell growth and invasion. In addition, Myr-AKT transfection reversed the expression of p-GSK-3β, β-catenin, N-cadherin, vimentin, c-Myc, cyclin D1, and E-cadherin, but not the expression of PGC-1α. These results suggest that down-regulation of p-AKT by PGC-1α knockdown occurs downstream of PGC-1α. We observed a direct physical interaction of PGC-1α with AKT in NC shRNA-SW620 cells and PGC-1α-SW480 cells, however this interaction was weaker in PGC-1α shRNA-SW620 cells and pcDNA-SW480 cells. These results suggest that interaction of PGC-1α and AKT may contribute to the regulation of AKT activity, even though the underlying molecular mechanisms remain to be clarified. In contrast to our observations, however, it has been shown that PGC-1α is phosphorylated by AKT and GSK-3β, resulting in both the inhibition of activity and the proteasomal degradation of PGC-1α (25, 26). These results suggest that the function of PGC-1α may be complex and depend on the cell type and its posttranslational modification. To our knowledge, this is the first report to show that PGC-1α knockdown inhibits the phosphorylation of AKT and GSK-3β in CRC cells. However, the molecular mechanism by which PGC-1α knockdown inhibits AKT/GSK-3β/β-catenin axis are unknown and require further investigation. To add further support to these findings, we also confirmed that PGC-1α overexpression enhances cell proliferation and invasion *via* the up-regulation of AKT/GSK-3β/β-catenin in SW480 cells. Based on our observations, we propose in Figure 6 a schematic showing the potential molecular mechanisms by which PGC-1α modulates cell proliferation and invasion.

In conclusion, this study revealed for the first time, that PGC-1α regulates cell proliferation and invasion *via* AKT/GSK-3β/β-catenin axis in human colorectal cancer cells. These results provide a basis for considering PGC-1α as a potential therapeutic target molecule in certain cancers. Further studies to investigate these findings in mouse xenograft models and 3D culture are required in the future.

Conflicts of Interest

The Authors declare that they have no conflicts of interest.

Authors' Contributions

SHY conducted all the experiments and drafted the manuscript under the supervision of JIP. JIP conceived the idea for this study, interpreted the results of experiments and wrote the manuscript. All Authors discussed the results and reviewed the manuscript prior to submission.

Acknowledgements

This study was supported by the Basic Science Research Program through the National Research Foundation of Korea (NRF) funded by the Ministry of Science, ICT & Future Planning (NRF-2017R1A2B4011428); and by the National Research Foundation of Korea (NRF) funded by the Korean Government (MSIP) (2016R1A5A2007009).

References

1 Siegel RL, Miller KD and Jemal A: Cancer Statistics, 2017. CA Cancer J Clin *67(1)*: 7-30, 2017. PMID: 28055103. DOI: 10.3322/caac.21387

2 Huang D, Sun W, Zhou Y, Li P, Chen F, Chen H, Xia D, Xu E, Lai M, Wu Y and Zhang H: Mutations of key driver genes in colorectal cancer progression and metastasis. Cancer Metastasis Rev *37(1)*: 173-187, 2018. PMID: 29322354. DOI: 10.1007/s10555-017-9726-5

3 Jones AW, Yao Z, Vicencio JM, Karkucinska-Wieckowska A and Szabadkai G: PGC-1 family coactivators and cell fate: roles in cancer, neurodegeneration, cardiovascular disease and retrograde mitochondria-nucleus signalling. Mitochondrion *12(1)*: 86-99, 2012. PMID: 21983689. DOI: 10.1016/j.mito.2011.09.009

4 Puigserver P, Wu Z, Park CW, Graves R, Wright M and Spiegelman BM: A cold-inducible coactivator of nuclear receptors linked to adaptive thermogenesis. Cell *92(6)*: 829-839, 1998. PMID: 9529258. DOI: 10.1016/s0092-8674(00)81410-5

5 Feilchenfeldt J, Bründler MA, Soravia C, Tötsch M and Meier CA: Peroxisome proliferator-activated receptors (PPARS) and associated transcription factors in colon cancer: Reduced expression of PPARγ-coactivator 1 (PGC-1). Cancer Lett *203(1)*: 25-33, 2004. PMID: 14670614. DOI: 10.1016/j.canlet.2003.08.024

6 Watkins G, Douglas-Jones A, Mansel R and Jiang W: The localisation and reduction of nuclear staining of PPARγ and PGC-1 in human breast cancer. Oncol Rep *12(2)*: 483-488, 2004. PMID: 15254719.

7 Zhang Y, Ba Y, Liu C, Sun G, Ding L, Gao S, Hao J, Yu Z, Zhang J, Zen K, Tong Z, Xiang Y and Zhang C: PGC-1α induces apoptosis in human epithelial ovarian cancer cells through a PPARγ-dependent pathway. Cell Res *17(4)*: 363-373, 2007. PMID: 17372612. DOI: 10.1038/cr.2007.11

8 Shiota M, Yokomizo A, Tada Y, Inokuchi J, Tatsugami K, Kuroiwa K, Uchiumi T, Fujimoto N, Seki N and Naito S: Peroxisome proliferator-activated receptor γ coactivator-1α interacts with the androgen receptor (AR) and promotes prostate cancer cell growth by activating the AR. Mol Endocrinol *24(1)*: 114-127, 2010. PMID: 19884383. DOI: 10.1210/me.2009-0302

9 Srivastava S, Barrett JN and Moraes CT: PGC-1α/β upregulation is associated with improved oxidative phosphorylation in cells harboring nonsense mtDNA mutations. Hum Mol Genet *16(8)*: 993-1005, 2007. PMID: 17341490. DOI: 10.1093/hmg/ddm045

10 Yun SH, Han SH and Park JI: Peroxisome proliferator-activated receptor γ and PGC-1α in cancer: Dual actions as tumor promoter and suppressor. PPAR Res *2018*: 6727421, 2018. PMID: 29599799. DOI: 10.1155/2018/6727421

11 Yun SH, Roh MS, Jeong JS and Park JI: Peroxisome proliferator-activated receptor γ coactivator-1α is a predictor of lymph node metastasis and poor prognosis in human colorectal cancer. Ann Diagn Pathol *33*: 11-16, 2018. PMID: 29566941. DOI: 10.1016/j.anndiagpath.2017.11.07

12 Shin SW, Yun SH, Park ES, Jeong JS, Kwak JY and Park JI: Overexpression of PGC-1α enhances cell proliferation and tumorigenesis of HEK293 cells through the upregulation of Sp1 and Acyl-CoA binding protein. Int J Oncol *46(3)*: 1328-1342, 2015. PMID: 25585584. DOI: 10.3892/ijo.2015.2834

13 Yun SH, Shin SW and Park JI: Expression of fatty acid synthase is regulated by PGC-1α and contributes to increased cell proliferation. Oncol Rep *38(6)*: 3497-3506, 2017. PMID: 29130104. DOI: 10.3892/or.2017.6044

14 White BD, Chien AJ and Dawson DW: Dysregulation of Wnt/β-catenin signalling in gastrointestinal cancers. Gastroenterology *142(2)*: 219-232, 2012. PMID: 22155636. DOI: 10.1053/j.gastro.2011.12.001

15 Novellasdemunt L, Antas P and Li VS: Targeting Wnt signaling in colorectal cancer. A review in the theme: cell signaling: proteins, pathways and mechanisms. Am J Physiol Cell Physiol *309(8)*: C511-C521, 2015. PMID: 26289750. DOI: 10.1152/ajpcell.00117.2015

16 De Craene B and Berx G: Regulatory networks defining EMT during cancer initiation and progression. Nat Rev Cancer *13(2)*: 97-110, 2013. PMID: 23344542. DOI: 10.1038/nrc3447

17 Ye B, Jiang LL, Xu HT, Zhou DW and Li ZS: Expression of PI3K/AKT pathway in gastric cancer and its blockcade suppresses tumor growth and metastasis. Int J Immunopathol Pharmacol *25(3)*: 627-636, 2012. PMID: 23058013. DOI: 10.1177/039463201202500309

18 Xu W, Yang Z and Lu N: A new role for the PI3K/Akt signaling pathway in the epithelial-mesenchymal transition. Cell Adh Migr *9(4)*: 317-324, 2015. PMID: 26241004. DOI: 10.1080/19336918.2015.1016686

19 Shin SW, Seo CY, Han H, Han JY, Jeong JS, Kwak JY and Park JI: 15d-PGJ_2 induces apoptosis by reactive oxygen species-mediated inactivation of Akt in leukemia and colorectal cancer cells and shows in vivo antitumor activity. Clin Cancer Res *15(17)*: 5414-5425, 2009. PMID: 19690198. DOI: 10.1158/1078-0432.CCR-08-3101

20 Hewitt RE, McMarlin A, Kleiner D, Werstro R, Martin P, Tsokos M, Stamp GW and Stetler-Stevenson WG: Validation of a model of colon cancer progression. J Pathol *192(4)*: 446-454, 2000. PMID: 11113861. DOI: 10.1002/1096-9896(2000)9999:9999<::AID-PATH775>3.0.CO;2-K

21 Bost F and Kaminski L: The metabolic modulator PGC-1α in cancer. Am J Cancer Res *9(2)*: 198-211, 2019. PMID: 30906622.

22 Wang P, Guo X, Zong W, Li Y, Liu G, Lv Y, Zhu Y and He S: PGC-1α/SNAI1 axis regulates tumor growth and metastasis by targeting miR-128b in gastric cancer. J Cell Physiol *234(10)*: 17232-17241, 2019. PMID: 30684287. DOI: 10.1002/jcp.28193

23 LeBleu VS, O'Connell JT, Gonzalez Herrera KN, Wikman H, Pantel K, Haigis MC, de Carvalho FM, Damascena A, Dominqos Chinen LT, Rocha RM, Asara JM and Kalluri R: PGC-1α mediates mitochondrial biogenesis and oxidative phosphorylation in cancer cells to promote metastasis. Nat Cell Biol *16(10)*: 992-1003, 2014. PMID: 25241037. DOI: 10.1038/ncb3039

24 Andrzejewski S, Klimcakova E, Johnson RM, Tabariès S, Annis MG, McGuirk S, Northey JJ, Chénard V, Sriram U, Papadopoli DJ and St-Pierre J: PGC-1α promotes breast cancer metastasis and confers bioenergetic flexibility against metabolic drugs. Cell Metab *26(5)*: 778-787, 2017. PMID: 28988825. DOI: 10.1016/j.cmet.2017.09.006

25 Li X, Monks B, Ge Q and Birnbaum MJ: Akt/PKB regulates hepatic metabolism by directly inhibiting PGC-1α transcription coactivator. Nature *447(7147)*: 1012-1016, 2007. PMID: 17554339. DOI: 10.1038/nature05861

26 Olson BL, Hock MB, Ekholm-Reed S, Wohlschlegel JA, Dev KK, Kralli A and Reed SI: SCFCdc4 acts antagonistically to the PGC-1α transcriptional coactivator by targeting it for ubiquitin-mediated proteolysis. Genes Dev *22(2)*: 252-264, 2008. PMID: 18198341. DOI: 10.1101/gad.1624208

Received December 17, 2019
Revised December 23, 2019
Accepted December 30, 2019